

# Coordination Behaviour of Bis-Terdentate N-Donor Ligands: Double- and Single-Stranded Helicates, Mesocates, and Cyclic Oligomers

Nawal K. Al-Rasbi,<sup>[a]</sup> Harry Adams,<sup>[a]</sup> Lindsay P. Harding,<sup>[b]</sup> and Michael D. Ward\*<sup>[a]</sup>

**Keywords:** Chelating ligands / Coordination chemistry / Helical structures / Self-assembly

Three new ligands have been prepared in which two terdentate chelating pyrazolyl-bipyridine units are connected by a central aromatic spacer via methylene "hinges": the spacers are *o*-phenylene (L<sup>Ph</sup>), 2,6-pyridine-diyl (L<sup>Py</sup>) and 2,3-naphthalenediyl (L<sup>Naph</sup>). The ligands act as potentially hexadentate bridging ligands, with the central pyridyl N atom of L<sup>Py</sup> not involved in coordination. The following complexes were prepared and structurally characterised: [M<sub>2</sub>(L<sup>Ph</sup>)<sub>2</sub>][ClO<sub>4</sub>]<sub>4</sub> (M = Ni, Cu), which are dinuclear double helicates; [Ag<sub>2</sub>(L<sup>Ph</sup>)(MeCN)<sub>2</sub>][BF<sub>4</sub>]<sub>2</sub>, a dinuclear complex with an Ag...Ag bond in which the ligand adopts a helical twist around the pair of metal ions; [Ni<sub>2</sub>(L<sup>Py</sup>)<sub>2</sub>][BF<sub>4</sub>]<sub>4</sub>, an achiral "mesocate" with a box-like structure and a face-to-face arrangement of

ligands; [Ag<sub>3</sub>(L<sup>Naph</sup>)<sub>2</sub>](BF<sub>4</sub>)<sub>3</sub>, which contains a linear trinuclear array of Ag<sup>I</sup> ions with the two ligands arranged in a shallow helical twist, each ligand spanning one terminal and the central metal ion; and [Cd<sub>6</sub>(L<sup>Naph</sup>)<sub>6</sub>](ClO<sub>4</sub>)<sub>12</sub>, a cyclic hexanuclear helicate with a perchlorate anion in the central cavity. Both [Cu<sub>2</sub>(L<sup>Ph</sup>)<sub>2</sub>][ClO<sub>4</sub>]<sub>4</sub> and [Cd<sub>6</sub>(L<sup>Naph</sup>)<sub>6</sub>](ClO<sub>4</sub>)<sub>12</sub>, which have architecturally similar bridging ligands, show evidence by electrospray mass spectrometry for formation of a range of cyclic oligomers in solution up to 11-mers for the Cd<sup>II</sup>/L<sup>Naph</sup> system.

(© Wiley-VCH Verlag GmbH & Co. KGaA, 69451 Weinheim, Germany, 2007)

## Introduction

Complexes with double or triple helical structures ("helicates") have been of interest in the field of coordination chemistry for many years. These assemblies have elegantly demonstrated how the formation of architecturally complex systems is directed by the interplay between simple parameters such as the stereoelectronic preference of the metals ion and the disposition of the binding sites in the ligand.<sup>[1]</sup>

Despite that the fact that very many helical complexes are known, the field remains as popular as ever because of the development of new research areas which involve them. These are remarkably diverse as some very recent examples will illustrate. Hannon and co-workers have shown how relatively simple dinuclear helicates bind to DNA and stabilise a triple junction.<sup>[2]</sup> Rice and co-workers have prepared ligands in which the degree of twist between the two binding domains can be controlled by allosteric means, allowing the assembly of helicate complexes to be controlled by an external perturbation.<sup>[3]</sup> A double helical ligand array has been used as a scaffold for a dinuclear Cu<sup>I</sup>/Cu<sup>II</sup> complex which shows unusual electronic delocalisation behaviour.<sup>[4]</sup> Piguet

has used polynuclear helicate complexes to understand and illustrate the phenomenon of cooperativity in self-assembly processes,<sup>[5]</sup> and has used heterodinuclear d/f helicates for studies on photoinduced energy-transfer between d-block and f-block luminophores.<sup>[6]</sup> Nitschke has used structurally relatively simple dinuclear Cu<sup>I</sup> helicates with different combinations of ligands to probe the concept of "valence frustration" which plays an important role in controlling self-assembly processes.<sup>[7]</sup> Triple helicates with a pendant hydrogen-bonding group attached to each ligand have been found to bind anions in the resultant pocket, and such anion binding can control the orientation of the three ligands in the helical scaffold.<sup>[8]</sup> Williams and co-workers showed how dinuclear helicates can display unusual stepwise spin-cross-over properties, associated with mechanical coupling between the two metal centres.<sup>[9]</sup> Certain anions can template formation of cyclic helicates in which the anion occupies the central cavity, and the size of the anion dictates the size of the metal/ligand circular helical array around it.<sup>[10]</sup>

We report here the preparation and coordination chemistry of a set of three new bis-terdentate ligands L<sup>Ph</sup>, L<sup>Py</sup>, and L<sup>Naph</sup> (Scheme 1), in which two terdentate arms, each based on a pyrazolyl-pyridyl-pyridyl sequence of donors, are connected to various different aromatic spacers (*o*-phenylene, pyridine-2,6-diyl, and 2,3-naphthalenediyl, respectively). Flexibility in the ligand backbone is provided by the methylene "hinges" which connect the terdentate arms to the central spacer. These belong to a general class of bridging

[a] Department of Chemistry, University of Sheffield,

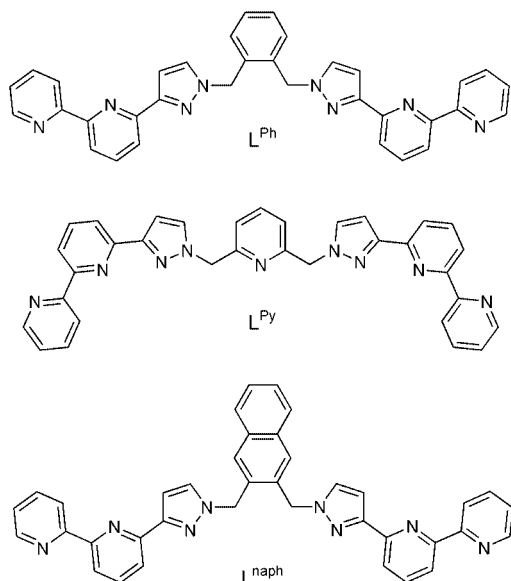
Sheffield S3 7HF, UK

Fax: +44-114-2229346

E-mail: m.d.ward@sheffield.ac.uk

[b] Department of Chemical and Biological Sciences, University of Huddersfield, Huddersfield HD1 3DH, UK

ligand that we have studied extensively in the last few years and which have proven to be particularly effective at providing polynuclear complexes with elaborate and often unexpected structures.<sup>[10b,11]</sup>



Scheme 1.

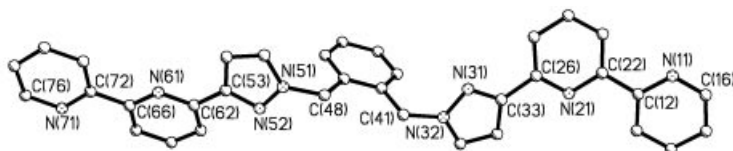
## Results and Discussion

### Ligand Syntheses

The new ligands (Scheme 1) were prepared by the reaction of two equivalents of 6-(pyrazol-3-yl)-2,2'-bipyridine<sup>[12]</sup> with the appropriate bis(bromomethyl)-substituted organic spacer, in the presence of hydroxide ion under phase-transfer conditions, according to the method we have used for related ligands in this series.<sup>[13]</sup> All of the spectroscopic and analytical data were consistent with the formulation of the ligands. Needles of  $L^{\text{Ph}}$  suitable for X-ray analysis were obtained by slow evaporation of a dilute dichloromethane solution of the ligand. The crystal structure is presented in Figure 1. Individual bond lengths and angles within the ligand are unremarkable. The crystal packing shows an extensive combination of weak  $\text{CH}\cdots\text{N}$  hydrogen bonds and  $\pi$ - $\pi$  stacking interactions between adjacent molecules.

### Complexes with $L^{\text{Ph}}$

Reaction of  $L^{\text{Ph}}$  with perchlorate salts of  $\text{Ni}^{\text{II}}$  or  $\text{Cu}^{\text{II}}$  in MeCN afforded crystalline products of empirical formula

Figure 1. Structure of  $L^{\text{Ph}}$ .

$\text{M}(\text{L}^{\text{Ph}})(\text{ClO}_4)_2$  by elemental analysis, that is 1:1  $\text{M}^{2+}/\text{L}^{\text{Ph}}$  stoichiometry. X-ray quality crystals could be grown for  $\text{M} = \text{Cu}$  and  $\text{Ni}$  by diffusion of diethyl ether vapour into MeCN solutions of the complexes.

Both complexes  $[\text{M}_2(\text{L}^{\text{Ph}})_2][\text{ClO}_4]_4$  ( $\text{M} = \text{Ni}, \text{Cu}$ ) proved to be dinuclear double helicates with two ligands wrapped around two metal ions; each ligand donates one terdentate site to each metal ion, and each metal ion is six-coordinate from coordination by two terdentate fragments, one from each ligand. Their gross structures are very similar (Figure 2), with minor differences arising from the distorted coordination environment around  $\text{Cu}^{\text{II}}$  due to the Jahn–Teller effect. Thus the  $\text{Ni}^{\text{II}}$  complex has fairly regular coordination around the  $\text{Ni}^{\text{II}}$  ions, with the  $\text{Ni}$ – $\text{N}$ (pyridine) bond lengths in the range 2.00–2.10 Å and the  $\text{Ni}$ – $\text{N}$ (pyrazole) distances being slightly longer at 2.12–2.18 Å. The angles between the two  $\text{Ni}(\text{NNN})$  planes at  $\text{Ni}(1)$  and  $\text{Ni}(2)$  are 92.5° and 94.2°, respectively (Table 1). Areas of overlap between aromatic rings on adjacent ligands are clear, resulting in some degree of stabilisation of the structure by  $\pi$ -stack-

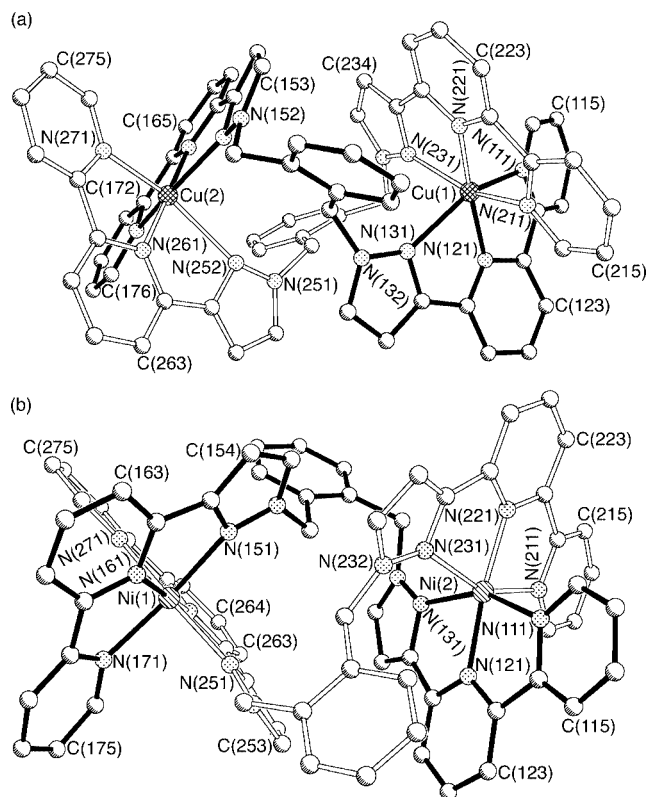


Figure 2. Structures of the double helical complex cations of (a)  $[\text{Cu}_2(\text{L}^{\text{Ph}})_2][\text{ClO}_4]_4 \cdot 2\text{MeCN} \cdot 0.5\text{H}_2\text{O}$  and (b)  $[\text{Ni}_2(\text{L}^{\text{Ph}})_2][\text{ClO}_4]_4 \cdot \text{MeCN}$ , with the ligands shaded differently for clarity.

Table 1. Selected bond lengths [Å] and angles [°] for  $[\text{Ni}_2(\text{L}^{\text{Ph}})_2][\text{ClO}_4]_4 \cdot \text{MeCN}$ .

Ni(1)–N(161)	2.001(4)	Ni(2)–N(221)	2.005(4)
Ni(1)–N(261)	2.008(4)	Ni(2)–N(121)	2.019(4)
Ni(1)–N(171)	2.102(4)	Ni(2)–N(211)	2.106(4)
Ni(1)–N(271)	2.110(4)	Ni(2)–N(111)	2.110(4)
Ni(1)–N(251)	2.118(4)	Ni(2)–N(131)	2.153(4)
Ni(1)–N(151)	2.164(4)	Ni(2)–N(231)	2.180(4)
N(161)–Ni(1)–N(261)	170.80(17)	N(221)–Ni(2)–N(121)	173.31(16)
N(161)–Ni(1)–N(171)	78.35(17)	N(221)–Ni(2)–N(211)	78.24(17)
N(261)–Ni(1)–N(171)	101.28(16)	N(121)–Ni(2)–N(211)	99.81(17)
N(161)–Ni(1)–N(271)	92.77(17)	N(221)–Ni(2)–N(111)	96.41(15)
N(261)–Ni(1)–N(271)	78.12(16)	N(121)–Ni(2)–N(111)	77.59(16)
N(171)–Ni(1)–N(271)	96.67(16)	N(211)–Ni(2)–N(111)	100.81(16)
N(161)–Ni(1)–N(251)	111.74(17)	N(221)–Ni(2)–N(131)	109.15(16)
N(261)–Ni(1)–N(251)	77.37(16)	N(121)–Ni(2)–N(131)	76.93(16)
N(171)–Ni(1)–N(251)	88.42(15)	N(211)–Ni(2)–N(131)	85.73(15)
N(271)–Ni(1)–N(251)	155.49(16)	N(111)–Ni(2)–N(131)	154.42(16)
N(161)–Ni(1)–N(151)	76.44(16)	N(221)–Ni(2)–N(231)	76.18(15)
N(261)–Ni(1)–N(151)	104.76(16)	N(121)–Ni(2)–N(231)	106.46(16)
N(171)–Ni(1)–N(151)	153.78(16)	N(211)–Ni(2)–N(231)	153.30(16)
N(271)–Ni(1)–N(151)	91.64(16)	N(111)–Ni(2)–N(231)	89.57(15)
N(251)–Ni(1)–N(151)	94.25(15)	N(131)–Ni(2)–N(231)	95.47(14)

Table 2. Selected bond lengths [Å] and angles [°] for  $[\text{Cu}_2(\text{L}^{\text{Ph}})_2][\text{ClO}_4]_4 \cdot 2\text{MeCN} \cdot 0.5\text{H}_2\text{O}$ .

Cu(1)–N(221)	1.973(4)	Cu(2)–N(161)	1.980(5)
Cu(1)–N(121)	2.007(5)	Cu(2)–N(261)	1.995(5)
Cu(1)–N(211)	2.115(6)	Cu(2)–N(171)	2.114(6)
Cu(1)–N(231)	2.170(5)	Cu(2)–N(271)	2.184(6)
Cu(1)–N(111)	2.233(5)	Cu(2)–N(151)	2.274(5)
Cu(1)–N(131)	2.355(7)	Cu(2)–N(252)	2.438(7)
N(221)–Cu(1)–N(121)	171.61(11)	N(161)–Cu(2)–N(261)	176.12(11)
N(221)–Cu(1)–N(211)	79.1(2)	N(161)–Cu(2)–N(171)	78.8(2)
N(121)–Cu(1)–N(211)	92.79(19)	N(261)–Cu(2)–N(171)	97.29(19)
N(221)–Cu(1)–N(231)	78.3(2)	N(161)–Cu(2)–N(271)	102.77(15)
N(121)–Cu(1)–N(231)	109.7(2)	N(261)–Cu(2)–N(271)	78.32(15)
N(211)–Cu(1)–N(231)	157.29(10)	N(171)–Cu(2)–N(271)	108.87(13)
N(221)–Cu(1)–N(111)	105.69(19)	N(161)–Cu(2)–N(151)	77.1(2)
N(121)–Cu(1)–N(111)	77.7(2)	N(261)–Cu(2)–N(151)	106.8(2)
N(211)–Cu(1)–N(111)	99.95(16)	N(171)–Cu(2)–N(151)	154.84(11)
N(231)–Cu(1)–N(111)	88.54(17)	N(271)–Cu(2)–N(151)	83.52(14)
N(221)–Cu(1)–N(131)	102.05(14)	N(161)–Cu(2)–N(252)	104.70(11)
N(121)–Cu(1)–N(131)	75.79(15)	N(261)–Cu(2)–N(252)	75.08(11)
N(211)–Cu(1)–N(131)	91.84(11)	N(171)–Cu(2)–N(252)	88.11(11)
N(231)–Cu(1)–N(131)	90.43(11)	N(271)–Cu(2)–N(252)	150.04(14)
N(111)–Cu(1)–N(131)	151.41(12)	N(151)–Cu(2)–N(252)	91.14(10)

ing. In the  $\text{Cu}^{\text{II}}$  complex in contrast the coordination geometry about the  $\text{Cu}^{\text{II}}$  ions is more distorted (Table 2). Cu(1) has a *trans*-related pair of Cu–N bonds from the same ligand (using a terminal pyridyl ring and the pyrazolyl ring) and that are significantly longer than the other four; for Cu(2) in contrast the distortion is expressed as an elongation of both Cu–N(pyrazolyl) bonds, which are *cis* to one another.

Electrospray mass spectra of both complexes revealed several peaks at the *m/z* values expected for the dinuclear complexes (see Experimental section). However in both cases there are very weak peaks identifiable whose *m/z* values are consistent with formation of higher oligomers. For redissolved crystals of  $[\text{Cu}_2(\text{L}^{\text{Ph}})_2][\text{ClO}_4]_4$  for example, the ES mass spectrum has a weak peak at *m/z* 979.1, assigned as  $\{\text{Cu}_4(\text{L}^{\text{Ph}})_4(\text{ClO}_4)_5\}^{3+}$ ; and redissolved crystals of  $[\text{Ni}_2(\text{L}^{\text{Ph}})_2][\text{ClO}_4]_4$  show numerous weak peaks at high *m/z*

values of which those at 972.4 and 1508.1 can be assigned as belonging to  $\{\text{Ni}_4(\text{L}^{\text{Ph}})_4(\text{ClO}_4)_5\}^{3+}$  and  $\{\text{Ni}_4(\text{L}^{\text{Ph}})_4(\text{ClO}_4)_6\}^{2+}$  respectively. Thus, both complexes which were isolated as dinuclear species in the solid state show evidence for traces of a tetrameric (presumably, cyclic helical) species existing in solution.<sup>[10]</sup>

Reaction of  $\text{L}^{\text{Ph}}$  with  $\text{AgBF}_4$  in MeCN, followed by diffusion of diisopropyl ether vapour into the solution, afforded crystals of  $[\text{Ag}_2(\text{L}^{\text{Ph}})(\text{MeCN})_2][\text{BF}_4]_2$  (Figure 3) which, in contrast to the two structures above, is a dinuclear *single* stranded helicate. The hexadentate ligand  $\text{L}^{\text{Ph}}$  is arranged in a shallow spiral which is wound around a central axis of two  $\text{Ag}^{\text{I}}$  ions; the two metals end up close enough together to be considered as having an argentophilic bond between them  $[\text{Ag}(1)\cdots\text{Ag}(2), 3.07 \text{ \AA}]$ . Somewhat surprisingly, the two  $\text{Ag}^{\text{I}}$  ions are in markedly different coordination environments. It might be expected [cf. the structures

with  $\text{Cu}^{\text{II}}$  and  $\text{Ni}^{\text{II}}$ , above] that  $\text{L}^{\text{Ph}}$  would donate a terdentate pyrazolyl-bipyridine arm to each  $\text{Ag}^{\text{I}}$  ion. Instead the partitioning of the ligand into two binding sites occurs within one of the terdentate units, such that one terdentate arm of the ligand donates only a bipyridyl unit to  $\text{Ag}(1)$ , with the adjacent pyrazolyl donor [N(51)] closer to  $\text{Ag}(2)$  (2.43 Å) than to  $\text{Ag}(1)$  (2.78 Å). Such ambiguous bridging interactions of a single N-donor ligand to a pair of  $\text{Ag}^{\text{I}}$  ions is known in other cases.<sup>[14]</sup> The remaining terdentate arm

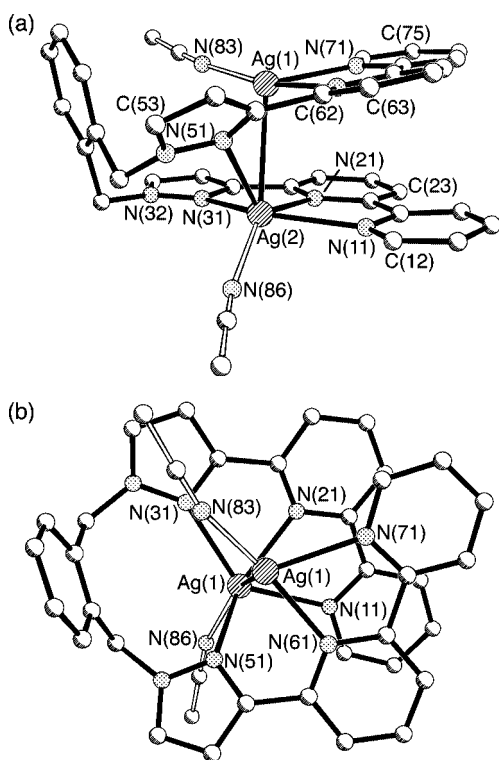


Figure 3. Structure of the complex cation of  $[\text{Ag}_2(\text{L}^{\text{Ph}})(\text{MeCN})_2][\text{BF}_4]_2$  (MeCN ligands are shown shaded differently for clarity).

Table 3. Selected bond lengths [Å] and angles [°] for  $[\text{Ag}_2(\text{L}^{\text{Ph}})(\text{MeCN})_2][\text{BF}_4]_2$ .

Ag(1)–N(71)	2.386(8)
Ag(1)–Ag(2)	3.0697(12)
Ag(2)–N(21)	2.344(7)
Ag(2)–N(86)	2.366(9)
Ag(2)–N(51)	2.428(7)
Ag(2)–N(11)	2.451(8)
Ag(2)–N(31)	2.514(8)
N(83)–Ag(1)–N(61)	167.3(3)
N(83)–Ag(1)–N(71)	112.1(3)
N(61)–Ag(1)–N(71)	70.6(3)
N(21)–Ag(2)–N(86)	143.5(3)
N(21)–Ag(2)–N(51)	129.5(2)
N(86)–Ag(2)–N(51)	84.2(3)
N(21)–Ag(2)–N(11)	68.9(3)
N(86)–Ag(2)–N(11)	91.1(3)
N(51)–Ag(2)–N(11)	104.9(3)
N(21)–Ag(2)–N(31)	68.9(3)
N(86)–Ag(2)–N(31)	120.4(3)
N(51)–Ag(2)–N(31)	105.9(2)
N(11)–Ag(2)–N(31)	137.5(2)

of the ligand is bound in its entirety to  $\text{Ag}(2)$ . Thus,  $\text{L}^{\text{Ph}}$  acts as a “2+4”-dentate donor [or, possibly, a “2.5+3.5” donor if N(51) is considered as genuinely bridging] to the two  $\text{Ag}^{\text{I}}$  centres, each of which also has one MeCN ligand. The differences in coordination number of  $\text{Ag}(1)$  and  $\text{Ag}(2)$  are reflected in significantly longer average Ag–N bond lengths around  $\text{Ag}(2)$  (see Table 3).

A consequence of the single-stranded helical structure is that the bipyridyl groups at each end of the ligand are overlapping and  $\pi$ -stacked with each other. This is emphasised in Figure 3(b). These two bipyridyl groups are near-parallel, and the separation between them is ca. 3.3 Å. It is convenient that the separation between the two  $\text{Ag}^{\text{I}}$  ions is almost exactly that required for aromatic ligands coordinated to them to have an optimal  $\pi$ -stacking separation.

### $\text{Ni}^{\text{II}}$ Complex with $\text{L}^{\text{Py}}$

Reaction of  $\text{L}^{\text{Py}}$  with  $\text{Ni}(\text{BF}_4)_2$  in a 1:1 ratio in nitromethane afforded, after crystallisation,  $[\text{Ni}_2(\text{L}^{\text{Py}})_2][\text{BF}_4]_4$  which has the structure of a box-like achiral complex, sometimes called a “*meso*-helicite” or “*mesocate*”,<sup>[15]</sup> in which the two ligands are side-by-side rather than twisted around one another (Figure 4, Table 4). This suits the coordination preference of  $\text{Ni}^{\text{II}}$  for octahedral geometry as it allows the

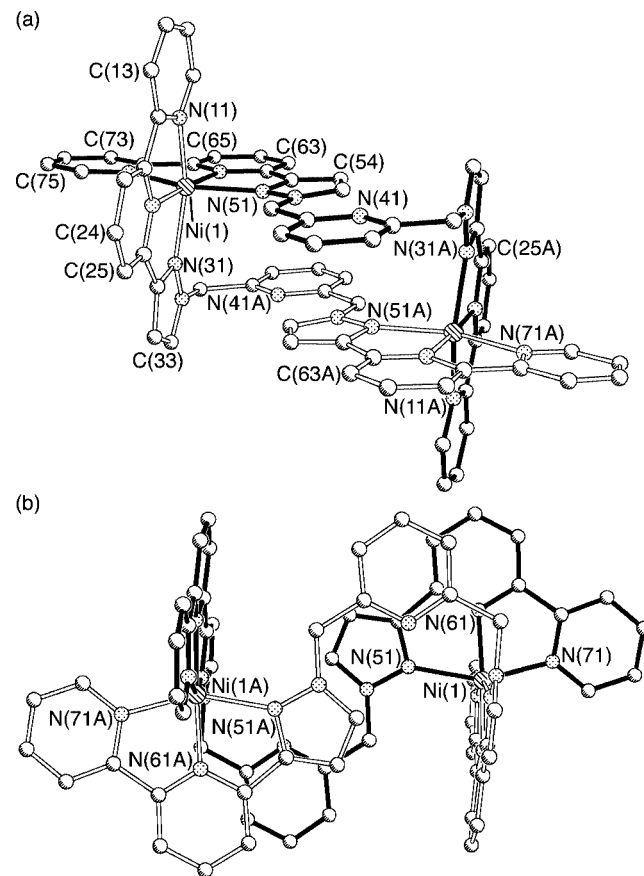


Figure 4. Two views of the complex cations of the mesocate  $[\text{Ni}_2(\text{L}^{\text{Py}})_2][\text{BF}_4]_4 \cdot 2\text{MeNO}_2$ , with the ligands shaded differently for clarity.

Table 4. Selected bond lengths [Å] and angles [°] for  $[\text{Ni}_2(\text{L}^{\text{Py}})_2][\text{BF}_4]_4 \cdot 2\text{MeNO}_2$ .

Ni(1)–N(21)	2.009(4)	Ni(1)–N(11)	2.094(4)
Ni(1)–N(61)	2.013(4)	Ni(1)–N(51)	2.154(4)
Ni(1)–N(71)	2.083(4)	Ni(1)–N(31)	2.172(4)
N(21)–Ni(1)–N(61)	177.12(16)	N(71)–Ni(1)–N(51)	154.70(15)
N(21)–Ni(1)–N(71)	104.50(15)	N(11)–Ni(1)–N(51)	90.63(15)
N(61)–Ni(1)–N(71)	78.20(16)	N(21)–Ni(1)–N(31)	76.77(15)
N(21)–Ni(1)–N(11)	78.17(16)	N(61)–Ni(1)–N(31)	102.26(14)
N(61)–Ni(1)–N(11)	102.85(16)	N(71)–Ni(1)–N(31)	92.46(15)
N(71)–Ni(1)–N(11)	92.20(15)	N(11)–Ni(1)–N(31)	154.89(15)
N(21)–Ni(1)–N(51)	100.68(14)	N(51)–Ni(1)–N(31)	95.56(14)
N(61)–Ni(1)–N(51)	76.66(15)		

two Ni(NNN) planes to be essentially perpendicular to one another ( $89^\circ$  between them), and also allows a region of overlap between parallel and overlapping ligand fragments in the space between the two metal ions, involving the pyrazolyl ring of one ligand [N(51)–C(55)] and the non-coordinated central pyridyl ring of the other [N(41A)–C(46A)], whose mean planes are separated by ca. 3.3 Å. The Ni–N bonds to the two pyrazolyl donors (average 2.16 Å) are slightly longer than to the four pyridyl donors (average 2.05 Å). Notably, the central pyridyl ring of each ligand [containing N(41)] does not participate in coordination but acts like a *meta*-phenylene spacer such that the ligand coordinated only via its terdentate pyrazolyl-bipyridine arms.

### Complexes with $\text{L}^{\text{naph}}$

This ligand is architecturally similar to  $\text{L}^{\text{Ph}}$  in that it has the same geometry spacer (an *ortho*-disubstituted six-membered aromatic ring) separating the two fragments. However, replacement of the 1,2-phenylene spacer by 2,3-naphthalenediyl spacer results in formation of some quite different structural types.

Reaction of  $\text{L}^{\text{naph}}$  with  $\text{AgBF}_4$  in MeCN afforded a clear solution, from which X-ray quality crystals were obtained following slow diffusion of diethyl ether vapour into the solution. The peak at the highest  $m/z$  value in the ES mass spectrum was at 1691.2, consistent with the 3:2 Ag/L fragment  $\{[\text{Ag}_3(\text{L}^{\text{naph}})_2][\text{BF}_4]_2\}^+$ , implying that the neutral

complex should be  $[\text{Ag}_3(\text{L}^{\text{naph}})_2](\text{BF}_4)_3$ . This was confirmed by X-ray crystallography; the structure is in Figure 5, and shows some interesting similarities to that of the simpler complex  $[\text{Ag}_2(\text{L}^{\text{Ph}})(\text{MeCN})_2][\text{BF}_4]_2$ . The trinuclear complex cation has  $C_2$  symmetry, and consists of a linear sequence of three  $\text{Ag}^{\text{I}}$  ions with two ligands each spanning two of them. Thus one ligand presents four of its six donor atoms (one entire tridentate arm, and the pyrazolyl donor of the next arm) to the terminal  $\text{Ag}^{\text{I}}$  ion, and the remaining two (a bipyridyl unit) to the next  $\text{Ag}^{\text{I}}$  at the centre of the array. We are seeing again how each ligand is partitioned into a “4+2-dentate” coordination mode rather than the more natural “3+3” mode which might be expected. The central  $\text{Ag}^{\text{I}}$  ion [Ag(1)] is therefore in a four-coordinate environment, connected to a terminal bipyridyl fragment from each of the two ligands; the terminal  $\text{Ag}^{\text{I}}$  ions are also four coordinate with all four donors coming from the same ligand (see Table 5). As with  $[\text{Ag}_2(\text{L}^{\text{Ph}})(\text{MeCN})_2][\text{BF}_4]_2$ , each ligand adopts a shallow monohelical twist such that the bipyridyl units at each end of a given ligand overlap with one another. The  $C_2$  symmetry of the complex cation means that both ligands have the same helical arrangement as one another, so the complex superstructure contains a pair of mono-helical ligands with the same configuration.

The  $\text{Ag}\cdots\text{Ag}$  separations are considerably higher than in dinuclear  $[\text{Ag}_2(\text{L}^{\text{Ph}})(\text{MeCN})_2][\text{BF}_4]_2$ , where it was 3.07 Å. Actually Ag(2) at the end of the sequence (and its symmetry equivalent at the other end) is disordered over two closely

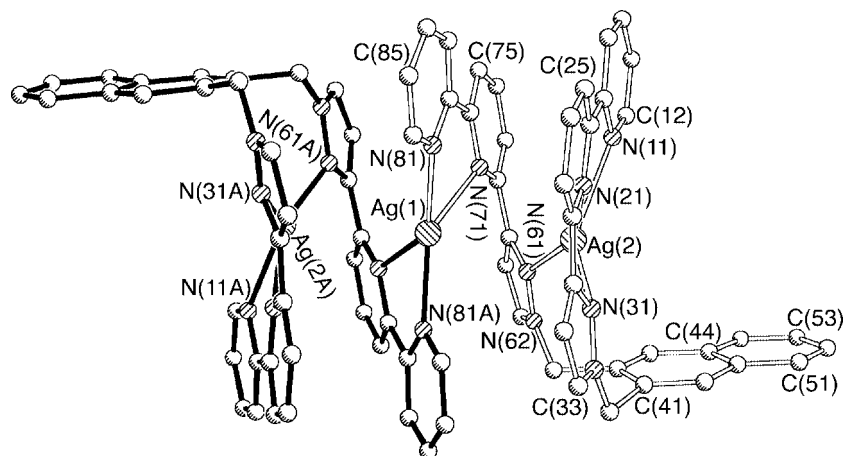


Figure 5. Structure of the complex cation of  $[\text{Ag}_3(\text{L}^{\text{naph}})_2](\text{BF}_4)_3 \cdot 2\text{MeCN}$ , with the two ligands shaded differently for clarity.

Table 5. Selected bond lengths [Å] and angles [°] for  $[\text{Ag}_3(\text{L}^{\text{naph}})_2](\text{BF}_4)_3 \cdot 2\text{MeCN}$ .

Ag(1)–N(81)	2.216(3)	Ag(2)–N(31) <sup>[b]</sup>	2.358(4)
Ag(1)–N(81)#1 <sup>[a]</sup>	2.216(3)	Ag(2)–N(11) <sup>[b]</sup>	2.571(4)
Ag(1)–N(71)#1	2.442(3)	Ag(3)–N(11) <sup>[c]</sup>	2.330(5)
Ag(1)–N(71)	2.442(3)	Ag(3)–N(61) <sup>[c]</sup>	2.360(4)
Ag(2)–N(61) <sup>[b]</sup>	2.234(3)	Ag(3)–N(21) <sup>[c]</sup>	2.454(4)
Ag(2)–N(21) <sup>[b]</sup>	2.249(4)	Ag(3)–N(31) <sup>[c]</sup>	2.590(4)
N(81)–Ag(1)–N(81)#1	149.64(16)	N(61)–Ag(2)–N(11)	111.63(13)
N(81)–Ag(1)–N(71)#1	133.99(10)	N(21)–Ag(2)–N(11)	67.05(14)
N(81)#1–Ag(1)–N(71)#1	71.15(10)	N(31)–Ag(2)–N(11)	130.67(13)
N(81)–Ag(1)–N(71)	71.15(10)	N(11)–Ag(3)–N(61)	116.11(14)
N(81)#1–Ag(1)–N(71)	133.99(10)	N(11)–Ag(3)–N(21)	67.96(15)
N(71)#1–Ag(1)–N(71)	89.64(14)	N(61)–Ag(3)–N(21)	130.54(19)
N(61)–Ag(2)–N(21)	154.59(11)	N(11)–Ag(3)–N(31)	131.13(15)
N(61)–Ag(2)–N(31)	117.07(12)	N(61)–Ag(3)–N(31)	104.52(15)
N(21)–Ag(2)–N(31)	72.34(13)	N(21)–Ag(3)–N(31)	65.20(13)

[a] Symmetry transformations used to generate equivalent atoms: #1  $-x + 2, y, -z + 1/2$ . [b] Ag(2) has a site occupancy of 58%. [c] Ag(3) has a site occupancy of 42%.

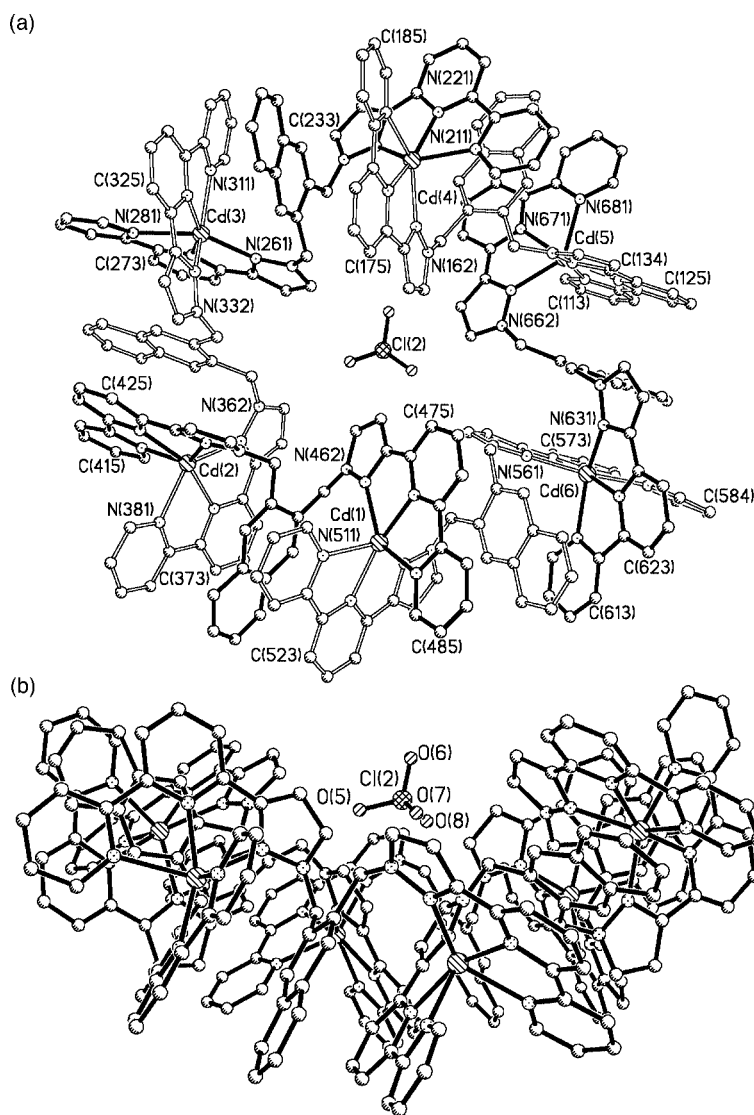


Figure 6. Two views of the structure of the complex cation of  $[\text{Cd}_6(\text{L}^{\text{naph}})_6](\text{ClO}_4)_{12}$ : (a) a face-on view, with the ligands shaded alternately dark and light for clarity, emphasising the cyclic helical structure and the encapsulated anion in the centre; (b) an edge-on view showing the shallow bowl shape of the cation.

spaced sites, with the Ag(1)⋯Ag(2) separation being 3.35 Å and Ag(1)⋯Ag(2') being 3.88 Å, such that argentophilic interactions are clearly much less significant than for [Ag<sub>2</sub>(L<sup>Ph</sup>)(MeCN)<sub>2</sub>][BF<sub>4</sub>]<sub>2</sub>. The structure of this complex may be compared with those of other linear polynuclear complexes of Ag<sup>I</sup> with polypyridine-type ligands.<sup>[16]</sup>

Reaction of L<sup>naph</sup> with Cd(ClO<sub>4</sub>)<sub>2</sub> in MeCN (1:1 ratio), followed by diffusion of diethyl ether vapour into the resultant solution, afforded X-ray quality colourless needles. On the basis of the common preference of Cd<sup>II</sup> for six-coordinate geometry, we were expecting a dinuclear double helicate to form similar to what we observed for [M<sub>2</sub>(L<sup>Ph</sup>)<sub>2</sub>][ClO<sub>4</sub>]<sub>4</sub> (M = Ni, Cu). Instead however the structure is that of a circular hexanuclear helicate [Cd<sub>6</sub>(L<sup>naph</sup>)<sub>6</sub>](ClO<sub>4</sub>)<sub>12</sub> (Figure 6), in which the 1:1 ratio of metal ions to ligands ensures that each Cd<sup>II</sup> centre is in a six-coordinate geometry (Cd–N separations lie in the range 2.21–2.41 Å, see Table 6). There are two significant non-covalent interactions involved, beyond the metal-ligand bonding, which appear to play a significant role in the structure. Firstly, each of the six naphthyl units is sandwiched between two pyridyl-pyrazole chelating units (from different ligands) to form a three-layer π-stack with separations of ca. 3.5 Å between the approximately parallel layers. Secondly, there is a perchlorate ion inside the ring which is involved in numerous short O⋯HC contacts with H atoms from the ligands. The anion is not actually centrally located in the cavity because the ring is not planar but slightly bowl-shaped; a view of the structure emphasising this is in Figure 6 (b).

Table 6. Selected bond lengths [Å] for [Cd<sub>6</sub>(L<sup>naph</sup>)<sub>6</sub>](ClO<sub>4</sub>)<sub>12</sub>.

Cd(1)–N(471)	2.301(7)	Cd(4)–N(221)	2.271(6)
Cd(1)–N(521)	2.305(6)	Cd(4)–N(171)	2.301(7)
Cd(1)–N(531)	2.325(7)	Cd(4)–N(231)	2.302(8)
Cd(1)–N(461)	2.331(6)	Cd(4)–N(161)	2.346(7)
Cd(1)–N(511)	2.334(6)	Cd(4)–N(211)	2.358(8)
Cd(1)–N(481)	2.371(7)	Cd(4)–N(181)	2.406(7)
Cd(2)–N(421)	2.294(6)	Cd(5)–N(131)	2.213(9)
Cd(2)–N(371)	2.312(6)	Cd(5)–N(121)	2.216(9)
Cd(2)–N(411)	2.325(7)	Cd(5)–N(661)	2.312(10)
Cd(2)–N(431)	2.343(8)	Cd(5)–N(671)	2.317(10)
Cd(2)–N(361)	2.349(7)	Cd(5)–N(681)	2.352(11)
Cd(2)–N(381)	2.357(6)	Cd(5)–N(111)	2.380(10)
Cd(3)–N(271)	2.229(8)	Cd(6)–N(571)	2.208(10)
Cd(3)–N(321)	2.288(7)	Cd(6)–N(631)	2.323(9)
Cd(3)–N(261)	2.295(7)	Cd(6)–N(611)	2.326(8)
Cd(3)–N(331)	2.309(7)	Cd(6)–N(561)	2.338(9)
Cd(3)–N(311)	2.363(6)	Cd(6)–N(621)	2.342(9)
Cd(3)–N(281)	2.474(9)	Cd(6)–N(581)	2.451(9)

Circular helicates have been reported by several groups<sup>[10,17]</sup> and, in addition to their appealing structures, can have two features of interest. Firstly, there is often an anion located in the centre of the cavity which has acted as a template to induce assembly of the metal/ligand array around it. Thus, use of a differently-sized templating anion can lead to a larger circular helicate containing more metal ions and more ligands in the peripheral assembly to accommodate a larger anion in the central cavity. Secondly, there can be a dynamic equilibrium in solution between differently-sized assemblies (M<sub>3</sub>L<sub>3</sub>, M<sub>4</sub>L<sub>4</sub>, M<sub>5</sub>L<sub>5</sub> etc.), even if

a single component crystallises preferentially such that solid-state studies indicate that only a single product has formed. Accordingly we examined the <sup>1</sup>H NMR spectrum and electrospray mass spectra of redissolved crystals of [Cd<sub>6</sub>(L<sup>naph</sup>)<sub>6</sub>](ClO<sub>4</sub>)<sub>12</sub>. The <sup>1</sup>H NMR spectrum in CD<sub>3</sub>CN showed no evidence for a mixture of species being present, with a clean spectrum being observed indicative of a structure with all ligands in a chiral twofold symmetric environment, viz. half of the ligand being unique, and the two CH<sub>2</sub> protons being inequivalent (diastereotopic) and coupled to one another (AB doublets) as a consequence of the chirality of the helicate.

The ES mass spectrum however reveals more complicated behaviour in solution that is not apparent from the <sup>1</sup>H NMR spectrum (Figure 7). The most intense peak at *m/z* 809.1 is ascribable to the mononuclear fragment {Cd(L<sup>naph</sup>)(ClO<sub>4</sub>)}<sup>+</sup>, implying either that dissociation of the complex occurs in solution, or that fragmentation occurs under mass spectroscopic conditions. The latter explanation is likely to be correct as the <sup>1</sup>H NMR spectrum shows that the main species in solution is chiral, i.e. at least a [Cd<sub>2</sub>(L<sup>naph</sup>)<sub>2</sub>]<sup>4+</sup> dinuclear double helicate. More interestingly, at higher *m/z* values are numerous much weaker peaks (< 2% of intensity of the main peak at *m/z* 809.1) whose *m/z* values match exactly to a range of oligomers ranging from a dimer [the peak at *m/z* 1717.2 corresponds to {Cd<sub>2</sub>(L<sup>naph</sup>)<sub>2</sub>(ClO<sub>4</sub>)<sub>3</sub>]<sup>4+</sup>, presumably a double helicate] up to an 11-mer [the peak at *m/z* 3229.2 corresponds to {Cd<sub>11</sub>(L<sup>naph</sup>)<sub>11</sub>(ClO<sub>4</sub>)<sub>9</sub>]<sup>2+</sup>, presumably a large cyclic helical assembly of the same nature as the crystal structure]. Altogether, peaks corresponding to {Cd(L<sup>naph</sup>)<sub>*n*</sub>} oligomers with *n* = 2, 4, 5, 7, 8, 10, 11 can be identified unambiguously; and a peak at *m/z* 2624.2 could correspond to either the *n* = 3 species {Cd<sub>3</sub>(L<sup>naph</sup>)<sub>3</sub>(ClO<sub>4</sub>)<sub>5</sub>]<sup>+</sup> or the *n* = 6 species {Cd<sub>6</sub>(L<sup>naph</sup>)<sub>6</sub>(ClO<sub>4</sub>)<sub>10</sub>]<sup>2+</sup> (or both, superimposed). It is clear that in solution an equilibrium mixture of cyclic helicates species exists.<sup>[10b]</sup> The fact that this is not apparent in the NMR spectrum implies either that they all have essentially

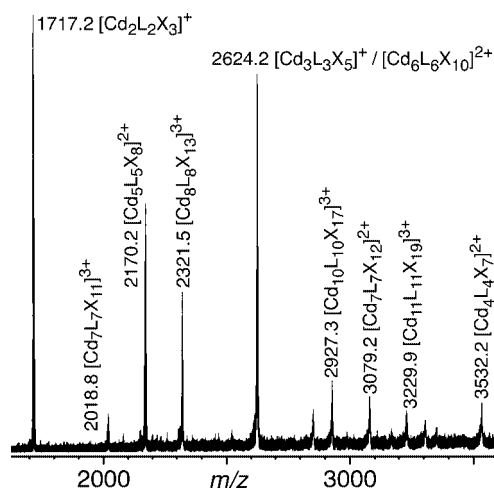


Figure 7. Part of the electrospray mass spectrum of redissolved crystals of [Cd<sub>6</sub>(L<sup>naph</sup>)<sub>6</sub>](ClO<sub>4</sub>)<sub>12</sub>, showing the presence of a range of cyclic oligomers in solution.

identical NMR spectra, or that one species is present in abundance and dominates the NMR spectrum, with the minor components being invisible. Either possibility is perfectly plausible.

A final interesting point about these complexes of  $L^{\text{naph}}$  is their luminescence spectra. The free ligand has a characteristic intense naphthalene-based fluorescence band at 347 nm. For the  $\text{Ag}^{\text{I}}$  complex  $[\text{Ag}_3(L^{\text{naph}})_2](\text{BF}_4)_3$  in MeCN solution, the fluorescence is reduced in intensity by about 90% but remains at exactly the same wavelength. In  $[\text{Cd}_6(L^{\text{naph}})_6](\text{ClO}_4)_{12}$  in MeCN solution however the fluorescence is significantly red-shifted, to 363 nm (Figure 8). We ascribe this to the extensive aromatic stacking of the emissive naphthyl units between pyridyl/pyrazolyl units of adjacent ligands in the cyclic helical array (see Figure 6), which results in stabilisation of the naphthyl-based  $\pi$ - $\pi^*$  excited state and hence a red-shift of the emission.<sup>[18]</sup> Even if other cyclic oligomers are present in solution, as the ES mass spectrum suggests, similar structures are plausible in which this type of stacking is retained. Thus the red-shifted luminescence of the ligand is indicative of the nature of the self-assembled structure formed in solution.

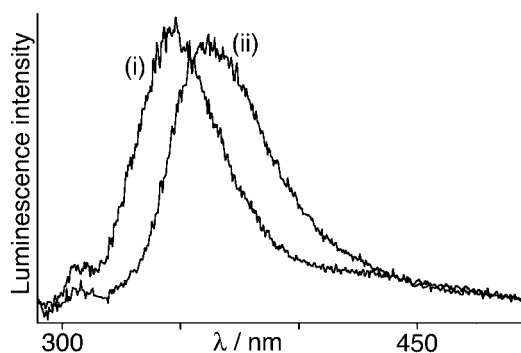


Figure 8. Luminescence spectra of solutions of (i)  $[\text{Ag}_3(L^{\text{naph}})_2](\text{BF}_4)_3$  and (ii)  $[\text{Cd}_6(L^{\text{naph}})_6](\text{ClO}_4)_{12}$  in MeCN, concentration ca.  $10^{-6}$  M; the solutions had the same optical density at the excitation wavelength.

## Conclusions

This series of relatively simple bridging ligands has generated a range of structures in which the ligands all span two metal ions – an essential prerequisite for formation of polynuclear assemblies – resulting in double helicates, a mesocate, some single-stranded helicates based on  $\text{Ag}^{\text{I}}$ , and a cyclic hexanuclear helicate based on  $\text{Cd}^{\text{II}}$ . In some cases there are obvious factors controlling the structures, such as the presence of  $\text{Ag}\cdots\text{Ag}$  interactions in the  $\text{Ag}^{\text{I}}$  complexes. In other cases apparently very similar metal/ligand combinations generate quite different structures, cf. the difference between the dinuclear double helicates  $[\text{M}_2(L^{\text{Ph}})_2][\text{ClO}_4]_4$  ( $\text{M} = \text{Ni}, \text{Cu}$ ) and the cyclic hexanuclear helicate  $[\text{Cd}_6(L^{\text{naph}})_6](\text{ClO}_4)_{12}$ ; both of these structural types have arisen from combination of bis-terdentate ligands (with similar spacers separating the binding sites) with six-coordinate metal ions. Significant factors favouring the formation

of  $[\text{Cd}_6(L^{\text{naph}})_6](\text{ClO}_4)_{12}$  could include the aromatic  $\pi$ -stacking between the naphthyl units, and the ability of  $\text{Cd}^{\text{II}}$  to tolerate a more highly distorted coordination environment than  $\text{Cu}^{\text{II}}$  or  $\text{Ni}^{\text{II}}$  on stereoelectronic grounds.

However, although it is tempting to try and rationalise such structural variations in a facile manner, it is not appropriate to over-do this for two reasons. Firstly, the number of variables involved is large: some of the more obvious factors include the charge and radius of the metal cation; stereoelectronic preferences arising from partially filled d-shells [for  $\text{Cu}^{\text{II}}$  and  $\text{Ni}^{\text{II}}$ ]; the presence of attractive  $\text{Ag}\cdots\text{Ag}$  interactions in the  $\text{Ag}^{\text{I}}$  complexes; the nature of the anion, which may exert a templating effect in the hexanuclear  $\text{Cd}^{\text{II}}$  circular helicate; and the presence of other supramolecular interactions such as aromatic  $\pi$ -stacking between ligands. Secondly, the solid-state structures are not necessarily thermodynamic minima but may represent kinetically stable assemblies which happened to crystallise well; for example the ES mass spectroscopic data for  $[\text{Cd}_6(L^{\text{naph}})_6](\text{ClO}_4)_{12}$  clearly shows that there is a mixture of oligomers in solution. Rationalising the appearance of one kinetic product in the solid state therefore does not tell the whole story.

## Experimental Section

**General Details:** 6-Acetyl-2,2'-bipyridine,<sup>[19]</sup> 6-(pyrazol-3-yl)-2,2'-bipyridine,<sup>[12]</sup> 2,6-bis(bromomethyl)pyridine,<sup>[20]</sup> and 2,3-bis(bromomethyl)naphthalene<sup>[21]</sup> were prepared as described previously. Other organic reagents and metal salts were obtained from Aldrich and Avocado and used as received. Instrumentation used for spectroscopic analysis were as follows:  $^1\text{H}$  NMR spectra, a Bruker AC 250 spectrometer. EI mass spectra, a VG AutoSpec magnetic sector instrument; ES mass spectra, a Bruker MicroTOF instrument in positive ion mode, with capillary exit and first skimmer voltages of 30 V and 60 V respectively. UV/Vis absorption spectra, a Cary 50 spectrophotometer, using MeCN solutions of the complexes.

### Syntheses of Ligands

**L<sup>Ph</sup>:** A mixture of 1,2-bis(bromomethyl)benzene (0.539 g, 2.04 mmol), 6-(pyrazol-3-yl)-2,2'-bipyridine (0.852 g, 3.84 mmol), 10 M aqueous NaOH (3 cm<sup>3</sup>),  $\text{NBU}_4\text{OH}$  (3 drops of 40% aqueous solution) and toluene (15 cm<sup>3</sup>) was heated with vigorous stirring to 85 °C for 24 h. After cooling, the organic layer was washed with water and then dried with  $\text{MgSO}_4$ . The solvent was removed to afford a pale yellow solid which was purified by column chromatography (5:95 EtOAc/ $\text{CH}_2\text{Cl}_2$  on alumina) to give 0.861 g (65%) of  $L^{\text{Ph}}$  as a white powder. EI MS:  $m/z$  (%) = 546 (3) [ $\text{M}^+$ ] and 324 (35) [ $\text{M}^+ - \text{pzbpy}$ ].  $^1\text{H}$  NMR (250 MHz,  $\text{CDCl}_3$ ):  $\delta$  = 8.67 (d, 2 H, bpy  $\text{H}^{6'}$ ), 8.57 (d, 2 H, bpy  $\text{H}^{3'}$ ), 8.33 (dd, 2 H, bpy  $\text{H}^3$ ), 8.01 (dd, 2 H, bpy  $\text{H}^5$ ), 7.76–7.85, (m, 4 H, bpy  $\text{H}^{5'}$  and  $\text{H}^{4'}$ ), 7.37 (d, 2 H, pz  $\text{H}^5$ ), 7.24–7.33 (m, 4 H, bpy  $\text{H}^4$  and phenyl  $\text{H}^3$  and  $\text{H}^4$ ), 7.17 (m, 2 H, phenyl  $\text{H}^2$  and  $\text{H}^5$ ), 7.07 (d, 2 H, pz  $\text{H}^4$ ) and 5.49 (s, 4 H,  $\text{CH}_2$ ) ppm.  $\text{C}_{34}\text{H}_{26}\text{N}_8$  (546.63): calcd. C 74.7, H 4.8, N 20.5; found C 74.9, H 4.7, N 20.3.

**L<sup>Pv</sup>:** A mixture of 2,6-bis(bromomethyl)pyridine (0.602 g, 2.27 mmol) and 6-(pyrazol-3-yl)-2,2'-bipyridine (1.00 g, 4.50 mmol) were reacted in exactly the same manner as described above for the synthesis of  $L^{\text{Ph}}$ . The crude product was purified by column chromatography (1% MeOH in  $\text{CH}_2\text{Cl}_2$ , on alumina) to give 0.593 g (47%) of  $L^{\text{Pv}}$  as yellow foam. EI MS:  $m/z$  (%) = 547

(5)  $[M^+]$  and 325 (100)  $[M^+ - \text{pzbpy}]$ .  $^1\text{H NMR}$  (250 MHz,  $\text{CDCl}_3$ ):  $\delta = 8.66$  (d, 2 H, bipy  $\text{H}^{6'}$ ), 8.58 (d, 2 H, bipy  $\text{H}^{3'}$ ), 8.32 (dd, 2 H, bipy  $\text{H}^3$ ), 8.02 (dd, 2 H, bipy  $\text{H}^5$ ), 7.83 (t, 4 H, bipy  $\text{H}^{4'}$  and  $\text{H}^{5'}$ ), 7.61–7.52 (m, 3 H, py  $\text{H}^3$ ,  $\text{H}^4$  and  $\text{H}^5$ ), 7.33 (t, 2 H, bipy  $\text{H}^4$ ), 7.11 (d, 2 H, pz  $\text{H}^5$ ), 6.93 (d, 2 H, pz  $\text{H}^4$ ) ppm.  $\text{C}_{33}\text{H}_{25}\text{N}_9 \cdot \text{H}_2\text{O}$  (565.63): calcd. C 70.1, H 4.8, N 22.3; found C 70.5, H 4.6, N 22.4.

**L<sup>naph</sup>**: A mixture of 2,3-bis(bromomethyl)naphthalene<sup>[9]</sup> (0.314 g, 1.00 mmol) and 6-(pyrazol-3-yl)-2,2'-bipyridine were reacted in the same manner as described above for the synthesis of  $\text{L}^{\text{Ph}}$ . The crude solid was purified by column chromatography (0.5% MeOH in  $\text{CH}_2\text{Cl}_2$ , on alumina) to give 0.390 g (69%) of yellow powder. EI-MS:  $m/z$  (%) = 596 (5)  $[M^+]$ , 374 (100)  $M^+ - \text{pzBipy}$ .  $^1\text{H NMR}$  (250 MHz,  $\text{CDCl}_3$ ):  $\delta = 8.65$  (d, 2 H, bipy  $\text{H}^{6'}$ ), 8.56 (d, 2 H, bipy  $\text{H}^{3'}$ ), 8.33 (dd, 2 H, bipy  $\text{H}^3$ ), 8.04 (dd, 2 H, bipy  $\text{H}^5$ ), 7.71–7.85, (m, 6 H, bipy  $\text{H}^{5'}$ ,  $\text{H}^{4'}$  and naphthyl  $\text{H}^5/\text{H}^8$ ), 7.59 (s, 2 H, naphthyl  $\text{H}^1/\text{H}^4$ ) 7.43–7.47 (m, 2 H, naphthyl  $\text{H}^6/\text{H}^7$ ), 7.43 (d, 2 H, pz  $\text{H}^5$ ), 7.24 (t, 2 H, bipy  $\text{H}^4$ ), 7.10 (d, 2 H, pz  $\text{H}^4$ ) and 5.56 (s, 4 H,  $\text{CH}_2$ ) ppm.  $\text{C}_{38}\text{H}_{28}\text{N}_8$  (596.69): calcd. C 76.5, H 4.7, N 18.8; found C 76.1, H 4.7, N 18.4.

### Syntheses of Complexes

Complexes were prepared by the reaction of the ligand (0.05 g) with the appropriate metal salt [in a 2:1 metal/ligand ratio for  $\text{Ag}^{\text{I}}$  complexes and in a 1:1 ratio for the  $\text{Ni}^{\text{II}}$ ,  $\text{Co}^{\text{II}}$ ,  $\text{Cu}^{\text{II}}$ , and  $\text{Cd}^{\text{II}}$  complexes] in nitromethane or acetonitrile. Diffusion of diisopropyl ether vapour into the resulting solutions afforded single crystals suitable for X-ray crystallography and other analyses. Characterisation data for the complexes are as follows.

**$[\text{Ni}_2\text{L}^{\text{Ph}}_2](\text{ClO}_4)_4$** : Yield: 0.050 g (68%). UV/Vis (MeCN):  $\lambda_{\text{max}}/\text{nm}$  ( $\epsilon$ ,  $\text{dm}^3 \text{mol}^{-1} \text{cm}^{-1}$ ) = 245 (32400), 260 (32600), 327 (18800), 340 (16700), 548 (29), 848 (71). ESMS:  $m/z$  = 704.1  $\{[\text{Ni}_2\text{L}^{\text{Ph}}_2](\text{ClO}_4)_2\}^{2+}$ , 436.4  $\{[\text{Ni}_2\text{L}^{\text{Ph}}_2](\text{ClO}_4)_3\}^{3+}$ , 302.6  $\{[\text{Ni}_2\text{L}^{\text{Ph}}_2]\}^{4+}$ .  $\text{Ni}_2\text{C}_{68}\text{H}_{52}\text{N}_{16}\text{Cl}_4\text{O}_{16} \cdot 2\text{H}_2\text{O}$  (1644.48): calcd. C 49.7, H 3.4, N 13.6; found C 49.3, H 3.5, N 13.6.

**$[\text{Cu}_2\text{L}^{\text{Ph}}_2](\text{ClO}_4)_4$** : Yield 0.046 g (62%). UV/Vis (MeCN):  $\lambda_{\text{max}}/\text{nm}$  ( $\epsilon$ ,  $\text{dm}^3 \text{mol}^{-1} \text{cm}^{-1}$ ) = 210 (67600), 245 (23000), 686 (69). ES MS:  $m/z$  = 1518.1  $\{[\text{Cu}_2\text{L}^{\text{Ph}}_2](\text{ClO}_4)_3\}^+$ , 979.1  $\{[\text{Cu}_4\text{L}^{\text{Ph}}_4](\text{ClO}_4)_5\}^{3+}$ ,

709.1  $\{[\text{Cu}_2\text{L}^{\text{Ph}}_2](\text{ClO}_4)_2\}^{2+}$ , 439.7  $\{[\text{Cu}_2\text{L}^{\text{Ph}}_2](\text{ClO}_4)_3\}^{3+}$ , 305.1  $\{[\text{Cu}_2\text{L}^{\text{Ph}}_2]\}^{4+}$ .  $\text{Cu}_2\text{C}_{68}\text{H}_{52}\text{N}_{16}\text{Cl}_4\text{O}_{16} \cdot 2\text{H}_2\text{O}$  (1654.19): calcd. C 49.4, H 3.4, N 13.5; found C 48.3, H 3.3, N 13.3.

**$[\text{Ag}_2\text{L}^{\text{Ph}}(\text{MeCN})_2](\text{BF}_4)_2$** : Yield 0.051 g (55%).  $^1\text{H NMR}$  (250 MHz,  $\text{CD}_3\text{CN}$ ):  $\delta = 8.06$  (d, 2 H, bipy  $\text{H}^{6'}$ ), 7.90–7.97 (m, 4 H, bipy  $\text{H}^{3'}$ ,  $\text{H}^3$ ), 7.75 (d, 2 H, bipy  $\text{H}^5$ ), 7.68 (d, 2 H, bipy  $\text{H}^{5'}$ ), 7.56 (d, 4 H, phenyl  $\text{H}^2$ ,  $\text{H}^3$ ), 7.53 (d, 2 H, pz  $\text{H}^5$ ), 7.44 (m, 2 H, py  $\text{H}^4$ ), 7.12 (dt, 2 H, py  $\text{H}^4$ ), 6.95 (d, 2 H, pz  $\text{H}^4$ ), 5.32 (s, 4 H,  $\text{CH}_2$ ) ppm. UV/Vis (MeCN):  $\lambda_{\text{max}}/\text{nm}$  ( $\epsilon$ ,  $\text{dm}^3 \text{mol}^{-1} \text{cm}^{-1}$ ) = 238 (40000), 265 (sh), 310 (19400). ES MS:  $m/z$  = 849.0  $\{[\text{Ag}_2\text{L}^{\text{Ph}}](\text{BF}_4)\}^+$ , 380.0  $\{[\text{Ag}_2\text{L}^{\text{Ph}}]\}^{2+}$ .  $\text{C}_{38}\text{H}_{32}\text{Ag}_2\text{B}_2\text{F}_8\text{N}_{10}$  (1018.07): calcd. C 44.8, H 3.2, N 13.8; found C 44.5, H 2.9, N 13.4.

**$[\text{Ni}_2\text{L}^{\text{Py}}_2](\text{BF}_4)_4$** : Yield 0.035 g (49%). UV/Vis (MeCN):  $\lambda_{\text{max}}/\text{nm}$  ( $\epsilon$ ,  $\text{dm}^3 \text{mol}^{-1} \text{cm}^{-1}$ ) = 247 (54800), 326 (19600), 845 (83). ES MS:  $m/z$  = 692.2  $\{[\text{Ni}_2\text{L}^{\text{Py}}_2](\text{BF}_4)_2\}^{2+}$ , 433.1  $\{[\text{Ni}_2\text{L}^{\text{Py}}_2](\text{BF}_4)_3\}^{3+}$ , 302.6  $\{[\text{Ni}_2\text{L}^{\text{Py}}_2]\}^{4+}$ . This sample was hygroscopic and gave variable elemental analyses consistent with the presence of several molecules of water per complex.

**$[\text{Ag}_3(\text{L}^{\text{naph}})_2](\text{BF}_4)_3$** : Yield 0.034 g (46%). UV/Vis (MeCN):  $\lambda_{\text{max}}/\text{nm}$  ( $\epsilon$ ,  $\text{dm}^3 \text{mol}^{-1} \text{cm}^{-1}$ ) = 227 (160000), 260 (89500), 310 (37100). ES MS:  $m/z$  = 1691.2  $\{[\text{Ag}_3(\text{L}^{\text{naph}})_2](\text{BF}_4)_2\}^+$ , 899.1  $\{[\text{Ag}_2(\text{L}^{\text{naph}})](\text{BF}_4)\}^+$ .  $\text{C}_{76}\text{H}_{56}\text{Ag}_3\text{B}_3\text{F}_{12}\text{N}_{16} \cdot 2\text{H}_2\text{O}$  (1813.42): calcd. C 50.3, H 3.3, N 12.4; found C 50.3, H 3.0, N 12.3.

**$[\text{Cd}_6(\text{L}^{\text{naph}})_6](\text{ClO}_4)_{12}$** : Yield 0.032 g (42%).  $^1\text{H NMR}$  (250 MHz,  $\text{CD}_3\text{CN}$ ):  $\delta = 8.44$  (d, 2 H, bipy  $\text{H}^{6'}$ ), 8.43 (br, 2 H, bipy  $\text{H}^3$ ), 8.29 (m, 2 H, bipy  $\text{H}^{3'}$ ), 8.28 (m, 2 H, bipy  $\text{H}^5$ ), 8.13 (s, 2 H, naphthyl  $\text{H}^1/\text{H}^4$ ), 7.99 (t, 2 H, bipy  $\text{H}^{5'}$ ), 7.95 (d, 2 H, naphthyl  $\text{H}^5/\text{H}^8$ ), 7.90 (d, 2 H, pz  $\text{H}^5$ ), 7.65–7.68 (2 H, naphthyl  $\text{H}^6/\text{H}^7$ ), 7.52 (dt, 2 H, bipy  $\text{H}^{4'}$ ), 7.31 (dt, 2 H, bipy  $\text{H}^{4'}$ ), 7.27 (dt, 2 H, pz  $\text{H}^4$ ), 5.38 (d, 2 H,  $\text{CH}_2$ ), 5.76 (d, 2 H,  $\text{CH}_2$ ) ppm. UV/Vis (MeCN):  $\lambda_{\text{max}}/\text{nm}$  ( $\epsilon$ ,  $\text{dm}^3 \text{mol}^{-1} \text{cm}^{-1}$ ) = 320 (22800), 268 (30200), 226 (55700). ES MS:  $m/z$  = 809.1  $\{[\text{Cd}(\text{L}^{\text{naph}})](\text{ClO}_4)\}^+$ , 1717.2  $\{[\text{Cd}_2(\text{L}^{\text{naph}})_2](\text{ClO}_4)_3\}^+$ , 2624.2  $\{[\text{Cd}_3(\text{L}^{\text{naph}})_3](\text{ClO}_4)_5\}^+$ , 3532.2  $\{[\text{Cd}_4(\text{L}^{\text{naph}})_4](\text{ClO}_4)_7\}^+$ , 1717.2  $\{[\text{Cd}_4(\text{L}^{\text{naph}})_4](\text{ClO}_4)_6\}^{2+}$ , 2170.2  $\{[\text{Cd}_5(\text{L}^{\text{naph}})_5](\text{ClO}_4)_8\}^{2+}$ , 2624.2  $\{[\text{Cd}_6(\text{L}^{\text{naph}})_6](\text{ClO}_4)_{10}\}^{2+}$ , 3079.2  $\{[\text{Cd}_7(\text{L}^{\text{naph}})_7](\text{ClO}_4)_{12}\}^{2+}$ ,

Table 7. Crystallographic data.

Complex	$\text{L}^{\text{Ph}}$	$[\text{Ni}_2(\text{L}^{\text{Ph}})_2](\text{ClO}_4)_4 \cdot \text{MeCN}$	$[\text{Cu}_2(\text{L}^{\text{Ph}})_2](\text{ClO}_4)_4 \cdot 2\text{MeCN} \cdot 0.5\text{H}_2\text{O}$	$[\text{Ag}_2(\text{L}^{\text{Ph}})(\text{MeCN})_2](\text{BF}_4)_2$
Empirical formula	$\text{C}_{34}\text{H}_{26}\text{N}_8$	$\text{C}_{70}\text{H}_{55}\text{Cl}_4\text{N}_{17}\text{Ni}_2\text{O}_{16}$	$\text{C}_{72}\text{H}_{59}\text{Cl}_4\text{Cu}_2\text{N}_{18}\text{O}_{16.5}$	$\text{C}_{38}\text{H}_{32}\text{Ag}_2\text{B}_2\text{F}_8\text{N}_{10}$
Formula mass	546.6	1649.53	1709.25	1018.1(0)
$T$ [K]	100(2)	150(2)	100(2)	150(2)
Crystal system, space group	monoclinic, $P2_1/n$	triclinic, $P\bar{1}$	triclinic, $P\bar{1}$	triclinic, $P\bar{1}$
$a$ [Å]	10.181(5)	13.6741(18)	13.73(4)	12.6315(16)
$b$ [Å]	23.562(12)	14.3285(19)	14.37(4)	13.1407(18)
$c$ [Å]	11.711(6)	21.426(3)	21.66(6)	13.6001(16)
$\alpha$ [°]	90	102.679(3)	102.22(5)	72.745(7)
$\beta$ [°]	95.079(16)	93.931(3)	94.69(3)	83.475(7)
$\gamma$ [°]	90	113.108(2)	112.83(4)	62.214(6)
$V$ [Å <sup>3</sup> ]	2798(2)	3710.5(9)	3786(17)	1906.4(4)
$Z$	4	2	2	2
$D_{\text{calcd}}$ [Mg/m <sup>3</sup> ]	1.298	1.476	1.499	1.774
$\mu$ [mm <sup>-1</sup> ]	0.081	0.730	0.783	1.112
Crystal size [mm]	0.14 × 0.06 × 0.04	0.32 × 0.14 × 0.09	0.27 × 0.20 × 0.07	0.35 × 0.16 × 0.08
Reflections collected	25235	32968	83182	43039
Independent reflections	4804 ( $R_{\text{int}} = 0.126$ )	13042 ( $R_{\text{int}} = 0.108$ )	14172 ( $R_{\text{int}} = 0.059$ )	6605 ( $R_{\text{int}} = 0.0333$ )
Data/restraints/parameters	4804/0/380	13042/5/982	14172/8/1020	6605/0/543
Final $R$ indices <sup>[a]</sup>	0.0576, 0.1518	0.0644, 0.1675	0.0456, 0.1199	0.0784, 0.1934
Largest diff. peak/hole [e Å <sup>-3</sup> ]	+0.22/−0.30	+0.77/−0.73	+0.92/−0.63	+2.42/−2.19

[a] The first value is  $R_1$ , based on “observed data” with  $I > 2\sigma(I)$ ; the second value is  $wR_2$ , based on all data.

Table 8. Crystallographic data.

Complex	[Ni <sub>2</sub> (L <sup>Py</sup> ) <sub>2</sub> ][BF <sub>4</sub> ] <sub>2</sub> ·2MeNO <sub>2</sub>	[Ag <sub>3</sub> (L <sup>naph</sup> ) <sub>2</sub> ](BF <sub>4</sub> ) <sub>3</sub> ·2MeCN	[Cd <sub>6</sub> (L <sup>naph</sup> ) <sub>6</sub> ](ClO <sub>4</sub> ) <sub>12</sub>
Empirical formula	C <sub>68</sub> H <sub>56</sub> B <sub>4</sub> F <sub>16</sub> N <sub>20</sub> Ni <sub>2</sub> O <sub>4</sub>	C <sub>80</sub> H <sub>62</sub> Ag <sub>3</sub> B <sub>3</sub> F <sub>12</sub> N <sub>18</sub>	C <sub>228</sub> H <sub>168</sub> Cd <sub>6</sub> Cl <sub>12</sub> N <sub>48</sub> O <sub>48</sub>
Formula mass	1681.98	1859.52	5447.90
<i>T</i> [K]	100(2)	100(2)	100(2)
Crystal system, space group	monoclinic, <i>P</i> 2 <sub>1</sub> / <i>n</i>	monoclinic, <i>C</i> 2/ <i>c</i>	monoclinic, <i>P</i> 2 <sub>1</sub> / <i>n</i>
<i>a</i> [Å]	12.3638(7)	15.1250(9)	25.350(2)
<i>b</i> [Å]	12.3036(7)	23.7334(15)	26.015(2)
<i>c</i> [Å]	23.4297(13)	20.9965(17)	41.398(3)
<i>α</i> [°]	90	90	90
<i>β</i> [°]	97.427(4)	103.930(3)	95.762(5)
<i>γ</i> [°]	90	90	90
<i>V</i> [Å <sup>3</sup> ]	3534.2(3)	7315.4(9)	27163(4)
<i>Z</i>	2	4	4
<i>D</i> <sub>calcd.</sub> [Mg/m <sup>3</sup> ]	1.581	1.688	1.332
<i>μ</i> [mm <sup>-1</sup> ]	0.641	0.887	0.654
Crystal size [mm]	0.18 × 0.16 × 0.14	0.06 × 0.04 × 0.03	0.24 × 0.16 × 0.06
Reflections collected	49325	55542	304166
Independent reflections	7161 ( <i>R</i> <sub>int</sub> = 0.0836)	8612 ( <i>R</i> <sub>int</sub> = 0.0546)	47783 ( <i>R</i> <sub>int</sub> = 0.1166)
Data/restraints/parameters	7161/4/514	8612/83/581	47783/1419/2197
Final <i>R</i> indices <sup>[a]</sup>	0.0680, 0.1934	0.0457, 0.1267	0.1195, 0.3615
Largest diff. peak/hole [e Å <sup>-3</sup> ]	+0.94/−0.72	+1.66/−1.01	+2.33/−1.38

[a] The first value is *R*<sub>1</sub>, based on “observed data” with *I* > 2σ(*I*); the second value is *wR*<sub>2</sub>, based on all data.

2018.8 {[Cd<sub>7</sub>(L<sup>naph</sup>)<sub>7</sub>](ClO<sub>4</sub>)<sub>11</sub>}<sup>3+</sup>, 3532.2 {[Cd<sub>8</sub>(L<sup>naph</sup>)<sub>8</sub>](ClO<sub>4</sub>)<sub>14</sub>}<sup>2+</sup>, 2321.5 {[Cd<sub>8</sub>(L<sup>naph</sup>)<sub>8</sub>](ClO<sub>4</sub>)<sub>13</sub>}<sup>3+</sup>, 2927.2 {[Cd<sub>10</sub>(L<sup>naph</sup>)<sub>10</sub>](ClO<sub>4</sub>)<sub>17</sub>}<sup>3+</sup>, 3229.2 {[Cd<sub>11</sub>(L<sup>naph</sup>)<sub>11</sub>](ClO<sub>4</sub>)<sub>19</sub>}<sup>3+</sup>. C<sub>228</sub>H<sub>168</sub>Cd<sub>6</sub>Cl<sub>12</sub>N<sub>48</sub>O<sub>48</sub>·10H<sub>2</sub>O (5628.19): calcd. C 48.7, H 3.4, N 11.9; found C 48.0, H 3.0, N 11.4.

### Crystallography

X-ray crystallographic data are summarised in Tables 7 and 8. In each case a suitable crystal was coated with hydrocarbon oil and attached to the tip of a glass fibre and transferred to a Bruker APEX-2 CCD diffractometer (graphite-monochromated Mo-*K*<sub>α</sub> radiation, λ = 0.71073 Å) under a stream of cold N<sub>2</sub>. After collection and integration the data were corrected for Lorentz and polarisation effects and for absorption by semi-empirical methods (SAD-ABS) based on symmetry-equivalent and repeated reflections.<sup>[22]</sup> The structures were solved by direct methods or heavy atom Patterson methods and refined by full-matrix least-squares methods on *F*<sup>2</sup>. Hydrogen atoms were placed geometrically and refined with a riding model and with *U*<sub>iso</sub> constrained to be 1.2 (1.5 for methyl groups) times *U*<sub>eq</sub> of the carrier atom. Structures were solved and refined using the SHELX suite of programs.<sup>[23]</sup> Significant bond lengths and angles for the structures of the metal complexes are in Tables 1–6. Particular problems associated with the refinements are as follows.

The complex cation of [Ni<sub>2</sub>(L<sup>Py</sup>)<sub>2</sub>][BF<sub>4</sub>]<sub>2</sub>·2MeNO<sub>2</sub> lies on an inversion centre with only one metal ion in the asymmetric unit. Crystals of [Cd<sub>6</sub>(L<sup>naph</sup>)<sub>6</sub>](ClO<sub>4</sub>)<sub>12</sub> scattered relatively weakly and only data with 2θ ≤ 50° were used in the final refinement. Several of the perchlorate anions showed disorder of the oxygen atoms which were in many cases disordered over two sites. Extensive use of geometric restraints was required to keep the Cl–O distances and the geometries of the perchlorate anions reasonable. Areas of electron density which presumably corresponded to disordered solvent molecules, but which could not be modelled as anything reasonable, were removed using the SQUEEZE command in PLATON. In [Ag<sub>3</sub>(L<sup>naph</sup>)<sub>2</sub>](BF<sub>4</sub>)<sub>3</sub>·2MeCN the complex cation lies on a twofold rotation axis which passes through Ag(1) and B(2). The “terminal” ion is disordered over two closely spaced sites [Ag(2), 58% site occupancy; Ag(3), 42% site occupancy]; only Ag(2) is shown in Figure 5. Some of the F atoms of the tetrafluoroborate ions are

disordered over two positions with the same fractional occupancies (0.58/0.42). None of the other structural determinations presented any significant problems.

CCDC-653275 to -653281 contain the supplementary crystallographic information for this paper. These data can be obtained free of charge from the Cambridge Crystallographic Data Centre via [www.ccdc.cam.ac.uk/data\\_request/cif](http://www.ccdc.cam.ac.uk/data_request/cif).

### Acknowledgments

We thank the Government of the Sultanate of Oman for a PhD studentship to N. K. A.

- [1] a) C. Piguet, G. Bernardinelli, G. Hopfgartner, *Chem. Rev.* **1997**, *97*, 2005; b) E. C. Constable, *Polynuclear Transition Metal Helicates*, in *Comprehensive Supramolecular Chemistry*, vol. 9 (Ed.: J.-P. Sauvage), Elsevier, Oxford, **1996**, p. 213; c) M. Albrecht, *Chem. Rev.* **2001**, *101*, 3457; d) M. J. Hannon, L. J. Childs, *Supramol. Chem.* **2004**, *16*, 7; e) A. F. Williams, *Chimia* **2000**, *54*, 585.
- [2] A. Oleksi, A. G. Blanco, R. Boer, I. Uson, J. Aymami, A. Rodger, M. J. Hannon, M. Coll, *Angew. Chem. Int. Ed.* **2006**, *45*, 1227.
- [3] T. Riis-Johannessen, L. P. Harding, J. C. Jeffery, R. Moon, C. R. Rice, *Dalton Trans.* **2007**, 1577.
- [4] J. C. Jeffery, T. Riis-Johannessen, C. J. Anderson, C. J. Adams, A. Robinson, S. P. Argent, M. D. Ward, C. R. Rice, *Inorg. Chem.* **2007**, *46*, 2417.
- [5] C. Piguet, M. Borkovec, J. Hamacek, K. Zeckert, *Coord. Chem. Rev.* **2005**, *249*, 705.
- [6] M. Cantuel, F. Gumy, J.-C. G. Bünzli, C. Piguet, *Dalton Trans.* **2006**, 2647.
- [7] J. R. Nitschke, *Acc. Chem. Res.* **2007**, *40*, 103.
- [8] a) L. P. Harding, J. C. Jeffery, T. Riis-Johannessen, C. R. Rice, Z. T. Zeng, *Chem. Commun.* **2004**, 654; b) L. P. Harding, J. C. Jeffery, T. Riis-Johannessen, C. R. Rice, Z. T. Zeng, *Dalton Trans.* **2004**, 2396.
- [9] S. G. Telfer, B. Bocquet, A. F. Williams, *Inorg. Chem.* **2001**, *40*, 4818.
- [10] a) C. S. Campos-Fernandez, B. L. Schottel, H. T. Chifotides, J. K. Bera, J. Basca, J. M. Koomen, D. H. Russell, K. R. Dun-

- bar, *J. Am. Chem. Soc.* **2005**, *127*, 12909; b) S. P. Argent, H. Adams, T. Riis-Johannessen, J. C. Jeffery, L. P. Harding, O. Mamula, M. D. Ward, *Inorg. Chem.* **2006**, *45*, 3905; c) P. L. Jones, K. J. Byrom, J. C. Jeffery, J. A. McCleverty, M. D. Ward, *Chem. Commun.* **1997**, 1361; d) B. Hasenknopf, J.-M. Lehn, B. O. Kneisel, G. Baum, D. Fenske, *Angew. Chem. Int. Ed. Engl.* **1996**, *35*, 1838; e) B. Hasenknopf, J.-M. Lehn, N. Boumediene, A. Dupont-Gervais, A. van Dorselaer, B. Kneisel, D. Fenske, *J. Am. Chem. Soc.* **1997**, *119*, 10956.
- [11] a) T. K. Ronson, H. Adams, L. P. Harding, S. J. A. Pope, D. Sykes, S. Faulkner, M. D. Ward, *Dalton Trans.* **2007**, 1006; b) S. P. Argent, H. Adams, T. Riis-Johannessen, J. C. Jeffery, L. P. Harding, W. Clegg, R. W. Harrington, M. D. Ward, *Dalton Trans.* **2006**, 4996; c) S. P. Argent, H. Adams, T. Riis-Johannessen, J. C. Jeffery, L. P. Harding, M. D. Ward, *J. Am. Chem. Soc.* **2006**, *128*, 72; d) S. P. Argent, H. Adams, L. P. Harding, M. D. Ward, *Dalton Trans.* **2006**, 542.
- [12] J. S. Fleming, E. Psillakis, S. M. Couchman, J. C. Jeffery, J. A. McCleverty, M. D. Ward, *J. Chem. Soc. Dalton Trans.* **1998**, 537.
- [13] Z. R. Bell, J. A. McCleverty, M. D. Ward, *Aust. J. Chem.* **2003**, *56*, 665.
- [14] E. R. Humphrey, Z. R. Reeves, J. C. Jeffery, J. A. McCleverty, M. D. Ward, *Polyhedron* **1999**, *18*, 1335.
- [15] T. K. Ronson, H. Adams, M. D. Ward, *New J. Chem.* **2006**, *30*, 26.
- [16] a) G. Baum, E. C. Constable, D. Fenske, C. E. Housecroft, T. Kulke, *Chem. Commun.* **1998**, 2659; b) G. Baum, E. C. Constable, D. Fenske, C. E. Housecroft, T. Kulke, M. Neuburger, M. Zehnder, *J. Chem. Soc. Dalton Trans.* **2000**, 945; c) S. Binsilong, J. D. Kildea, W. C. Patalinghug, B. W. Skelton, A. H. White, *Aust. J. Chem.* **1994**, *47*, 1545; d) L. Hou, D. Li, *Inorg. Chem. Commun.* **2005**, *8*, 128; e) M. J. Hannon, C. L. Painting, E. A. Plummer, L. J. Childs, N. W. Alcock, *Chem. Eur. J.* **2002**, *8*, 2225; f) C. Provent, S. Hewage, G. Brand, G. Bernardinelli, L. J. Charbonnière, A. F. Williams, *Angew. Chem. Int. Ed. Engl.* **1997**, *36*, 1287.
- [17] a) G. Baum, E. C. Constable, D. Fenske, C. E. Housecroft, T. Kulke, *Chem. Commun.* **1999**, 195; b) F. Tuna, J. Hamblin, A. Jackson, G. Clarkson, N. W. Alcock, M. J. Hannon, *Dalton Trans.* **2003**, 2141; c) O. Mamula, A. von Zelewsky, P. Brodard, C. W. Schlappfer, G. Bernardinelli, H. Stoeckli-Evans, *Chem. Eur. J.* **2005**, *11*, 3049.
- [18] N. K. Al-Rasbi, C. Sabatini, F. Barigelletti, M. D. Ward, *Dalton Trans.* **2006**, 4769.
- [19] E. C. Constable, F. Heirtzler, M. Neuburger, M. Zehnder, *J. Am. Chem. Soc.* **1997**, *119*, 5606.
- [20] H. Scheytza, O. Rademacher, H.-U. Reißig, *Eur. J. Org. Chem.* **1999**, 2373.
- [21] C. Wang, H. I. Mosberg, *Tetrahedron Lett.* **1995**, *36*, 3623.
- [22] G. M. Sheldrick: *SADABS*, A program for absorption correction with the Siemens SMART area-detector system, University of Göttingen, **1996**.
- [23] G. M. Sheldrick: *SHELXS-97* and *SHELXL-97*, programs for crystal structure solution and refinement, University of Göttingen, **1997**.

Received: July 9, 2007

Published Online: August 29, 2007